Geophysical Research Letters

Supporting Information for

Distinct ultrafine- and accumulation-mode particle properties in clean and polluted urban environments

Yuying Wang[1, 2], Zhanqing Li[3], Renyi Zhang[4], Xiaoai Jin[2], Weiqi Xu[5], Xinxin Fan[2], Hao Wu[2], Fang Zhang[2], Yele Sun[5], Qiuyan Wang[1], Maureen Cribb[3], Dawei Hu[5]

[1]School of Atmospheric Physics, Nanjing University of Information Science and Technology, Nanjing 210044, China
[2]State Key Laboratory of Earth Surface Processes and Resource Ecology, College of Global Change and Earth System Science, Beijing Normal University, Beijing 100875, China
[3]ESSIC and the Department of Atmospheric and Oceanic Science, University of Maryland, College Park, MD 20740, USA
[4]Department of Atmospheric Sciences and Department of Chemistry, Center for Atmospheric Chemistry and Environment, Texas A&M University, College Station, Texas 77843, United States
[5]State Key Laboratory of Atmospheric Boundary Layer Physics and Atmospheric Chemistry, Institute of Atmospheric Physics, Chinese Academy of Sciences, Beijing 100029, China
[6]School of Earth and Environmental Sciences, University of Manchester, Manchester, UK

Contents of this file

Introduction

Text S1.

Figure S1a shows mean GF-PDFs during this campaign. All particles with different sizes have two modes (the LH and MH modes). The LH-mode particles are mainly from primary emissions, and the MH-mode particles are mainly from secondary formation or the aging of primary particles (Fig. S1b). The difference in the peak GF values between 40- and 80–200-nm particles suggests different chemical compositions between them, implying different sources for particles of these two sets of particles.

Text S2.

The particle number size distribution (PNSD) is important to investigate aerosol sources in the atmosphere. This is because different emissions and chemical processes produce different sized particles (Peng et al., 2014). Figures S2a and S2b showed different diurnal evolutions of PNSD during clean and polluted conditions. The peak diameter variations of the main modes in the PNSD show that the main particle growth occurred in the afternoon during clean periods and in the morning and at night during polluted periods. This suggests different particle formation and growth processes during clean and polluted periods. During clean periods, the photochemical reaction is most important, so the main growth of newly formed particles occurs in the afternoon. During polluted periods, the aqueous reaction is most important, so the main growth of newly emitted particles occurs in the morning and at night when emissions are strong, and the ambient relative humidity (RH) is high (Fig. S3). To further illustrate this difference, the diurnal evolution of the ratio between clean to polluted period PNSDs was analyzed (Fig. S2c). The number concentration ratio between clean and polluted periods ($R_{clean/pollution}$) below 50 nm is always larger than 1, and the diameter range ($R_{clean/pollution} > 1$) expands obviously after 10:00 LT when nucleation events burst. This indicates more ultrafine-mode particles during clean periods through photochemical reactions.

PNSDs can be fitted using different mode lognormal distributions (Hussein et al., 2005; Peng et al., 2014). The lognormal distribution fitting shows two main modes (nucleation and Aitken modes) during clean periods and three main modes (nucleation, Aitken, and accumulation modes) during polluted period (Fig. S2e-f). The 40-nm particles are mainly in the nucleation and Aitken modes, and the 150-nm particles are mainly in the accumulation mode.

Text S3.

The PNSD at ambient RH was calculated using the measured dry number size distributions and the size-resolved hygroscopic growth factors at ambient RH. The size-resolved hygroscopic

growth factors were retrieved from size-resolved κ based on κ-Köhler theory (Bian et al., 2014). The ambient aerosol surface area can then be calculated using the ambient PNSD. Figure S5 shows the diurnal variations in ambient aerosol surface area during clean and polluted periods.

Text S4.

Figure S6 shows diurnal variations in trace gas mixing ratios during clean and polluted periods. High concentrations of ozone (O_3) during clean periods indicates a high atmospheric oxidation capacity, which is the result of photochemical reactions. The mixing ratios of other pollution trace gases (such as NO_x and SO_2) are much higher during polluted periods than clean periods. The high concentration of reactant gases is the reason why particle growth is rapid during polluted periods through aqueous reactions.

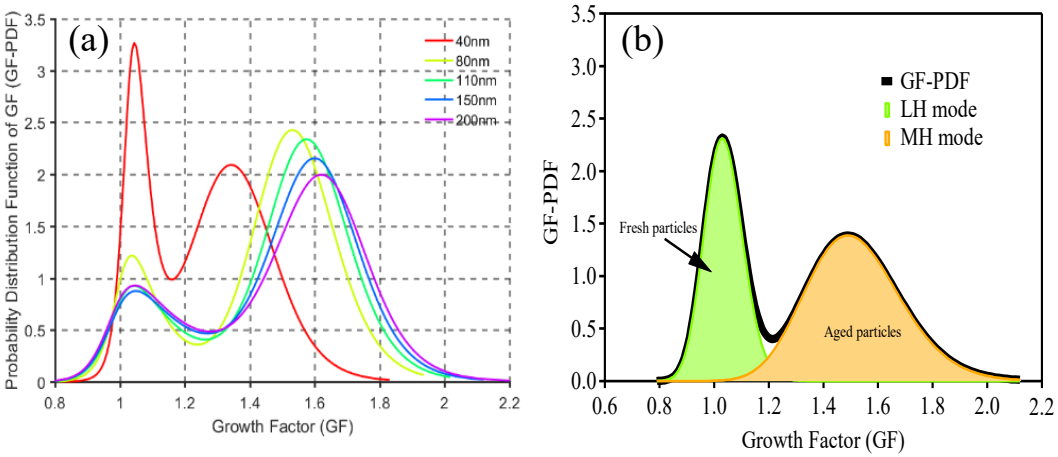

Figure S1. (a) Mean probability density functions of GF (GF-PDF) for different particle sizes derived from H-TDMA data and measured at RH = 90 % during the APHH field campaign, and (b) one typical GF-PDF case and its two hygroscopic modes.

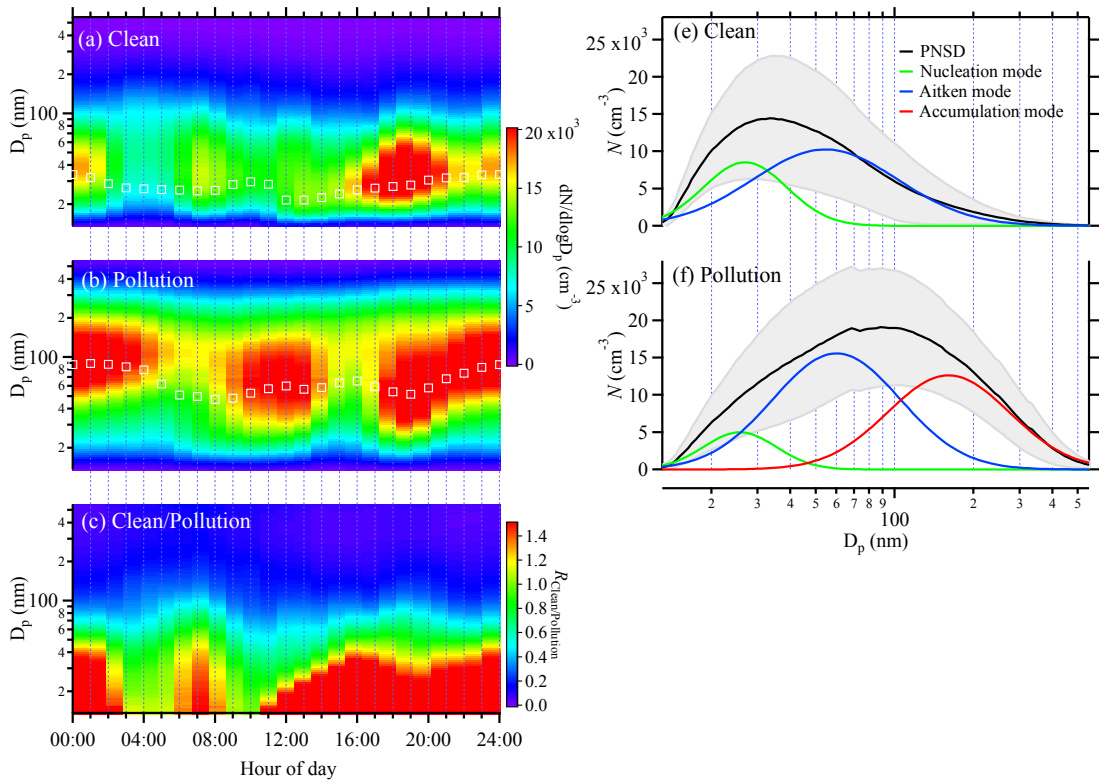

Figure S2. Diurnal variations in particle number size concentration (PNSD) during (a) clean and (b) polluted periods, and (c) their ratio. The mean PNSD (with standard deviations shown as shaded by gray areas) and its fitting lines during (e) clean and (f) polluted periods. The black squares in (a) and (b) are the peak diameters of the main modes in the PNSDs (nucleation mode during clean periods and Aitken mode during polluted periods).

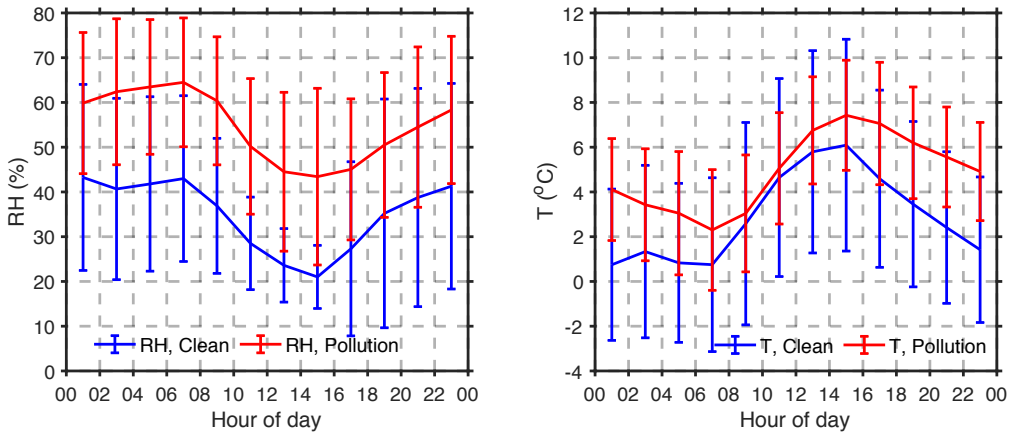

Figure S3. Diurnal variations in ambient relative humidity (RH, left panel) and temperature (T, right panel) measured at 8 m above ground level with standard deviations shown. The clean case is shown in blue, and the polluted case is shown in red.

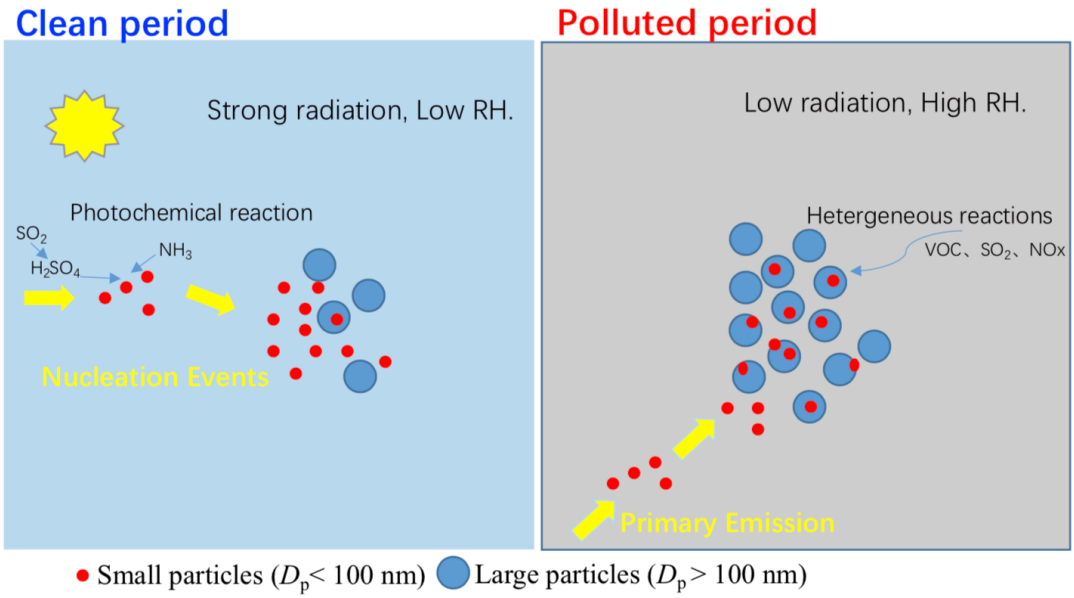

Figure S4. Schematic representation of the main chemical processes for ultrafine- (< 100 nm) and accumulation-mode (> 100 nm) particles during clean (left panel) and polluted (right panel) periods.

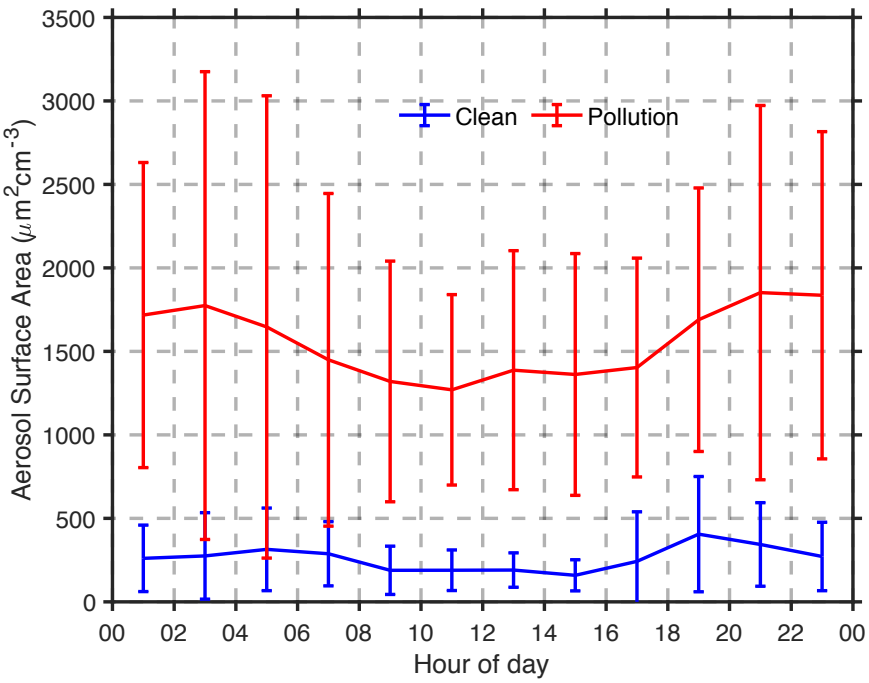

Figure S5. Diurnal variations in ambient aerosol surface area during clean and polluted periods.

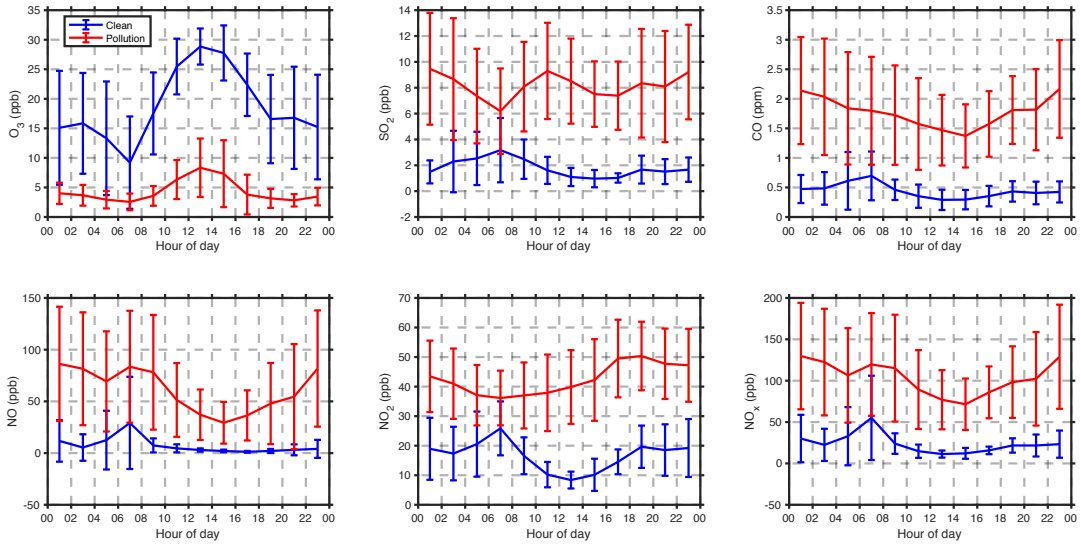

Figure S6. Diurnal variations of trace gas mixing ratios during clean and polluted periods. The clean case is shown in blue, and the polluted case is shown in red.

References

Bian Y. X., Zhao C. S., Ma N., Chen J. & Xu W. Y. (2014): A study of aerosol liquid water content based on hygroscopicity measurements at high relative humidity in the North China Plain, *Atmospheric Chemistry and Physics*, 14, 6417–6426, https://doi.org/10.5194/acp-14-6417-2014.

Hussein, T., Maso M. D., Petäjä T., Koponen I. K., Paatero P., Aalto P. P., Hämeri K., & Kulmala M. (2005), Evaluation of an automatic algorithm for fitting the particle number size distributions, *Boreal Environment Research*, *10*(5), 337–355.

Peng, J. F., Hu, M., Wang, Z. B., Huang, X. F., Kumar, P., Wu, Z. J., et al. (2014), Submicron aerosols at thirteen diversified sites in China: size distribution, new particle formation and corresponding contribution to cloud condensation nuclei production, *Atmospheric Chemistry and Physics*, *14*(18), 10,249–10,265, https://doi.org/doi:10.5194/acp-14-10249-2014.